ACOUSTIC WAVES GENERATED BY A LASER POINT SOURCE IN AN ISOTROPIC CYLINDER

Y. Pan[+], C. Rossignol[#], and B. Audoin[#]

+Institute of Acoustics, Tongji University, 200092, Shanghai, P. R. China
Laboratoire de Mécanique Physique UMR CNRS 8469, Université Bordeaux 1, Bordeaux, France
y.pan@lmp.u-bordeaux1.fr

Abstract

The acoustic field of a homogeneous and isotropic cylinder generated by a laser point source in either ablation or thermoelastic regime is obtained theoretically. A three-dimensional Fourier transform is used to calculate the acoustic displacement at the cylinder surface. Experimental waveforms were measured and analyzed for either regime. Experimental and theoretical normal displacements under thermoelastic regime are compared for aluminum cylinders. Very good agreements are observed in the time, shape and relative amplitude (i) of the cylindrical Rayleigh waves with different roundtrips, and (ii) of the various longitudinal and transverse bulk waves propagating through the cylinder or reflected at the free circular surface.

Introduction

There is an increasing demand of nondestructively evaluating cylindrical parts. Understanding the wave propagation in a cylinder is a necessary step before considering any possible application. Moreover, a cylinder with its unique geometry is a basic target for the acoustic wave propagation research.

Surface acoustic wave propagating on an isotropic and homogenous cylinder was studied in 1967 by Viktorov[1]. Higher Rayleigh-type waves were termed as "Whispering-gallery modes" by Ubell in 1973[2]. Due to the coupling difficulty of conventional piezoelectric transducers, few experimental reports on the wave propagation for a curved medium had been published until the development of the laser ultrasonic technique[3], in which ultrasonic waves are both generated and detected by lasers. With the remarkable features of non-contact, high spacious and temporal resolutions introduced by this technique, various studies on materials of curved surfaces have been carried out. As an example, Rayleigh wave propagating on a sphere was observed experimentally in 1988[4]. The finite element method has been used to predict the bulk and surface wave propagations when laser beam was focused by a cylindrical lens[5].

Very recently, authors have published a model[6] to predict the bulk and surface wave propagations in a transversely isotropic cylinder under either ablation or thermoelastic generation regime. The laser pulse was focused by a cylindrical lens, and the laser was represented by a transient line source. But the model can only predict the wave propagation within the isotropic plane perpendicular to the z axis, and the propagation along the z axis is still not studied. In this paper, a theoretical solution is presented to predict the acoustic field generated by a laser point source in either ablation or thermoelastic regime for a homogenous and isotropic cylinder. The wave propagation along the z axis is studied. Calculated waveforms of the normal displacement component are compared with experimental signals measured by the laser ultrasonic technique.

Statement of the problem

Consider a homogenous and isotropic cylinder of infinite length, radius a, and density ρ, with its axis of symmetry coinciding with the z-axis of its cylindrical coordinates (r, θ, z). Let λ and μ denote the two independent elastic constants. The components of the displacement vector depend on three spatial variables r, θ, z and on time t. These components, denoted as u_r, u_θ, and u_z can be written as[7]:

$$\begin{cases} u_r(r,\theta,z,t) = \dfrac{\partial \varphi}{\partial r} + a\dfrac{\partial^2 \psi}{\partial r \partial z} + \dfrac{1}{r}\dfrac{\partial \chi}{\partial \theta} \\[2mm] u_\theta(r,\theta,z,t) = \dfrac{1}{r}\dfrac{\partial \varphi}{\partial \theta} + \dfrac{a}{r}\dfrac{\partial^2 \psi}{\partial \theta \partial z} - \dfrac{\partial \chi}{\partial r} \\[2mm] u_z(r,\theta,z,t) = \dfrac{\partial \varphi}{\partial z} - a\left(\dfrac{\partial^2 \psi}{\partial r^2} + \dfrac{\partial \psi}{r \partial r} + \dfrac{\partial^2 \psi}{r^2 \partial \theta^2}\right) \end{cases} \quad (1)$$

where the three scalar potentials φ, ψ, and χ are governed by the waves motion equations

$$\begin{cases} \nabla^2 \varphi = \dfrac{\rho}{\lambda + 2\mu}\dfrac{\partial^2 \varphi}{\partial t^2} \\[2mm] \nabla^2 \psi = \dfrac{\rho}{\mu}\dfrac{\partial^2 \psi}{\partial t^2} \\[2mm] \nabla^2 \chi = \dfrac{\rho}{\mu}\dfrac{\partial^2 \chi}{\partial t^2} \end{cases} \quad (2)$$

and by either of the following boundary conditions. For a source at position $\theta=0°$, components σ_{rr}, $\sigma_{r\theta}$, and σ_{rz} of the stress tensor at any point of the surface are determined by either

$$\begin{cases} \sigma_{rr}\big|_{r=a} = -F_0\delta(t)\delta(z)\sum_{n=-\infty}^{+\infty}\delta(\theta - 2n\pi) \\[2mm] \sigma_{r\theta}\big|_{r=a} = 0 \\[2mm] \sigma_{rz}\big|_{r=a} = 0 \end{cases} \quad (3)$$

for the ablation generation[8], or

$$\begin{cases} \sigma_{rr}\big|_{r=a} = 0 \\[2mm] \sigma_{r\theta}\big|_{r=a} = -F_0 h(t)\delta(z)\sum_{n=-\infty}^{+\infty}\delta'(\theta - 2n\pi) \\[2mm] \sigma_{rz}\big|_{r=a} = -F_0 a h(t)\delta'(z)\sum_{n=-\infty}^{+\infty}\delta(\theta - 2n\pi) \end{cases} \quad (4)$$

for the thermoelastic generation[9]. In Eqs. (3) and (4), F_0 is a certain loading in N·µs·m^{-2} related to the laser pulse, and n stands for the number of clockwise ($n>0$) or anticlockwise ($n<0$) roundtrips of the generated acoustic waves. Here a delta function of time $\delta(t)$ and a Heaviside step function of time $h(t)$ are used for the ablation and thermoelastic generations, respectively; $\delta'(\theta - 2n\pi)$ denotes the derivative of the delta function $\delta(\theta - 2n\pi)$, and $\delta'(z)$ denotes the derivative of the delta function $\delta(z)$. In Eq. (3), a delta force is

postulated in time and space to represent sudden normal loading in the ablation regime. A Heaviside step function in time is considered in the thermoelastic regime [Eq. (4)] since thermal diffusion is neglected. Owing to the interface, a dipolar force is considered in Eq. (4) for the source shape.

Transformed solutions

The three-dimensional Fourier transform of the displacement field over the coordinate θ, z, and time t is now considered, and it is noted U_i ($i=r$, θ, or z). On noting $v=k_\theta a$, where k_θ is the component of the wave vector $\boldsymbol{k}$ along θ direction, three components of the displacement at a given surface position and time are then as follows

$$u_i(a,\theta,z,t) = (2\pi)^{-3}$$
$$\iiint_{-\infty}^{+\infty} U_i(a,v,k,\omega)e^{-j(v\theta+kz-\omega t)}\,dvdkd\omega \tag{5}$$

Here k is the component of the wave vector $\boldsymbol{k}$ along z direction.

Doing so, the wave motion equations and the boundary equations can be linearized, providing explicit forms for the potentials φ, ψ, and χ under either generation regime. Normal component of the displacement at the boundary are then obtained for ablation regime

$$U_r(a,v,k,\omega) = -\frac{F_0 a}{2\mu D(v,k,\omega)} \tag{6}$$

$$\{A_1 B_L - jkaA_2 B_T - jvA_3\}\sum_{n=-\infty}^{+\infty}e^{jv2n\pi}$$

and for thermoelastic regime

$$U_r(a,v,k,\omega) = \frac{F_0 aH(w)}{2\mu D(v,k,\omega)} \tag{7}$$

$$\{T_1 B_L - jkaT_2 B_T - jvT_3\}\sum_{n=-\infty}^{+\infty}e^{jv2n\pi}$$

where

$$\begin{cases} B_L = \beta a J'_v(\beta a)/J_v(\beta a) \\ B_T = \gamma a J'_v(\gamma a)/J_v(\gamma a) \\ \beta = \sqrt{k_L^2 - k^2} \\ \gamma = \sqrt{k_T^2 - k^2} \end{cases} \tag{8}$$

$$\begin{cases} A_1 = (m_{22}m_{33} - m_{23}m_{32}) \\ A_2 = (m_{23}m_{31} - m_{21}m_{33}) \\ A_3 = (m_{21}m_{32} - m_{22}m_{31}) \end{cases} \tag{9}$$

$$\begin{cases} T_1 = jv(m_{13}m_{32} - m_{33}m_{12}) + jka(m_{12}m_{23} - m_{22}m_{13}) \\ T_2 = jv(m_{11}m_{33} - m_{31}m_{13}) + jka(m_{21}m_{13} - m_{11}m_{23}) \\ T_3 = jv(m_{31}m_{12} - m_{11}m_{32}) + jka(m_{11}m_{22} - m_{21}m_{12}) \end{cases} \tag{10}$$

$$m_{ij} =$$
$$\begin{pmatrix} v^2 + (k^2 - \gamma^2)a^2/2 - B_L & -jka(v^2 - \gamma^2 a^2 - B_T) & jv(1-B_T) \\ jv(1-B_L) & vka(1-B_T) & \gamma^2 a^2/2 - v^2 + B_T \\ -jkaB_L & (k_T^2/2 - k^2)a^2 B_T & -vka/2 \end{pmatrix}$$
$$\tag{11}$$

Note that in Eqs. (8) and (11), $k_L = \omega\sqrt{\rho/(\lambda+2\mu)}$ and $k_T = \omega\sqrt{\rho/\mu}$ are the scalar wave vector of the longitudinal and transverse waves, respectively. In Eqs. (6) and (7), $D(v,k,\omega) = \det(m_{ij})$ is the determinate of the matrix m_{ij} [Eq. (11)]. Additionally, $H(\omega)$ is the Fourier transform of $h(t)$, and $J'_v(x)$ is the derivative of the Bessel function $J_v(x)$.

Now, let us focus on the calculation of the three-dimensional integral in Eq. (5). When dealing with an elastic material, this integrand shows discontinuities for a particular set of ω, v, and k values. They correspond to poles associated with the zeros of the dispersion equation

$$D(v,k,\omega) = 0. \tag{12}$$

For $k=0$, Eq. (12) yields to

$$\left(v^2 - k_T^2 a^2/2\right)^2 - v^2 + \left(1 - v^2\right)B_L B_T$$
$$+ k_T^2 a^2(B_L + B_T)/2 = 0 \tag{13}$$

that is identical to D_v in the Eq. (8) of Ref. 6 is null. These poles describe the cylindrical Rayleigh waves[1] and Whispering Gallery waves[2]. The integration thus appears to be not consistent with the Fourier transform. A suited numerical integration method should, therefore, be applied. For each value of the angular frequency ω, the two-dimensional integral on the real axes of the variable v and k is calculated by the method suggested by Weaver[10]. In this scheme, the Fourier transform is generalized by replacing ω by a complex variable ω-$j\delta$ with a small, constant and imaginary part δ. With this change of variable, Eq. (5) becomes

$$u_i(a,\theta,z,t) = \frac{e^{\delta t}}{8\pi^3}$$
$$\iiint_{-\infty}^{+\infty} U_i(a,v,k,\omega-j\delta)e^{-j(v\theta+kz-\omega t)}\,dvdkd\omega \tag{10}$$

The benefit of this method is twofold: (*i*) it preserves the application of the fast Fourier transform algorithms for the final inversion, and (*ii*) the two-dimensional integrand is a nonsingular function that may now be integrated numerically. To perform the numerical integration, the value δ=0.01 rad·μs^{-1} has been chosen for the auxiliary parameter in the following numerical calculations.

Results

The calculated normal displacements are compared to the experimental signals for aluminum cylinders under point source generations. A Nd:YAG laser is used for ultrasonic wave generation in either ablation
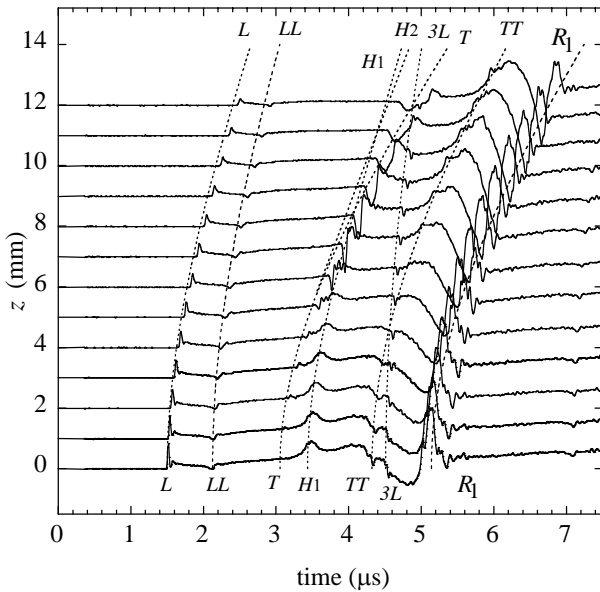
FIG. 1. Waterfall plots of experimental displacements under ablation generation at z=0, 1, …, and 12 mm for an aluminum cylinder ($2a$=9.62 mm).

or thermoelastic regime. The collimated optical beam is focused by means of a spherical lens (focus length is 150 mm). The diameter of the laser spot size is about 0.2 mm. The normal displacements were measured at the surface by using an optical heterodyne probe[4] with a power output of 100 mW and with a sensitivity of 10^{-14} m/$\sqrt{\text{Hz}}$.

Ablation regime

First let us look at the acoustic waves measured under ablation generation. The experimental signals generated by the laser point source are detected at z=0, 1, …, and 12 mm for an aluminum rod with a diameter $2a$=9.62 mm. Here the observation angle is 180°. As shown in Fig. 1, the waterfall plot of these waveforms clearly reveals various wave modes (see marked symbols). The direct longitudinal (L) and the once reflected longitudinal (LL) waves are clearly observable. The direct transverse (T) and the once reflected transverse (TT) waves are also observable. Their arrival times (displayed as dash lines in Fig. 1) are identical to their corresponding ray trajectories shown in Fig. 2(a). The first roundtrip of the cylindrical Rayleigh wave (R_1) is clearly observable. Its arrival time is in agreement with that of the ray trajectory shown in Fig. 2(b). Moreover, the twice reflected longitudinal wave ($3L$) is observed, and its ray trajectory is found in Fig. 2(c). A head wave (H_1) is observed, and its arrival time is identical to the corresponding ray trajectory in Fig. 2(b). Another head wave (H_2) is also observed, and its ray trajectory is found in Fig. 2(d).
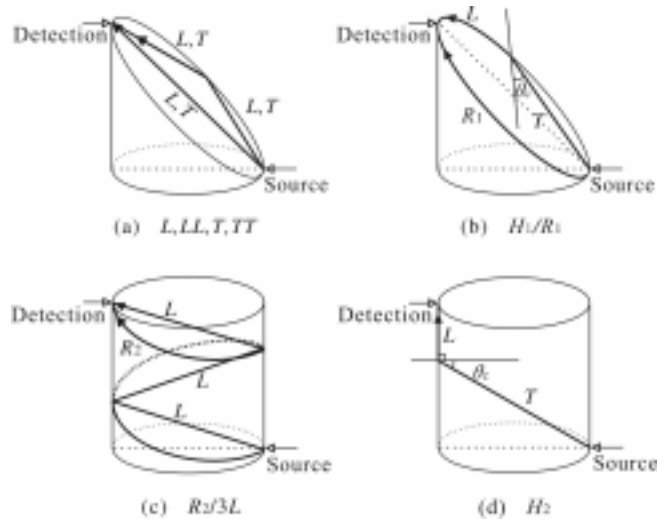

FIG. 2. Ray trajectories of L, LL, T, TT, H_1, R_1, R_2, $3L$, and H_2 waves observed in Figs. 1, 3-5. Here θ_c is the critical angle for aluminum rods.

Thermoelastic regime

Now let us look at the acoustic waves measured under thermoelastic generation. The experimental signals generated by the laser point source are detected at z=0, 2, …, and 14 mm for the same aluminum rod. The observation angle is 180°. As shown in Fig. 3, the waterfall plot of these waveforms also clearly reveals various wave modes. The L, LL, $3L$, and TT waves were observed under the ablation generation (Fig. 1), whereas they are not easily visible under this thermoelastic generation. This can be explained by the different directivities of the two generations[3]. The flying paths of H_1 and R_1 waves are along the corresponding ray trajectories shown in Fig. 2.
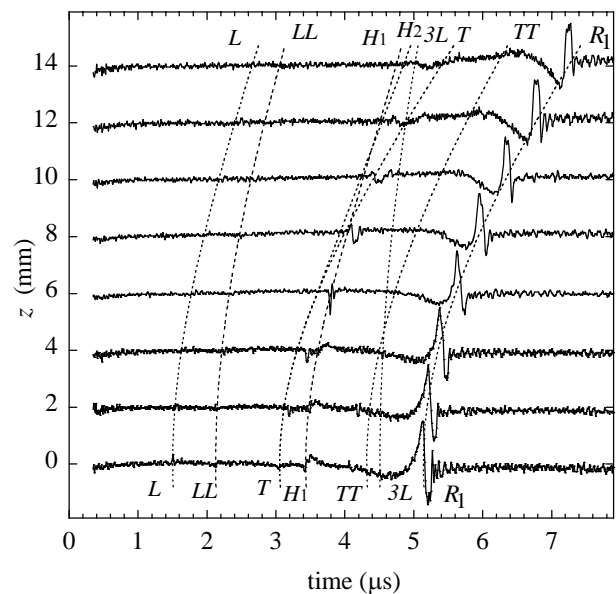

FIG. 3. Waterfall plots of experimental displacements under thermoelastic generation at z=0, 2, …, and 14 mm for an aluminum cylinder ($2a$=9.62 mm).
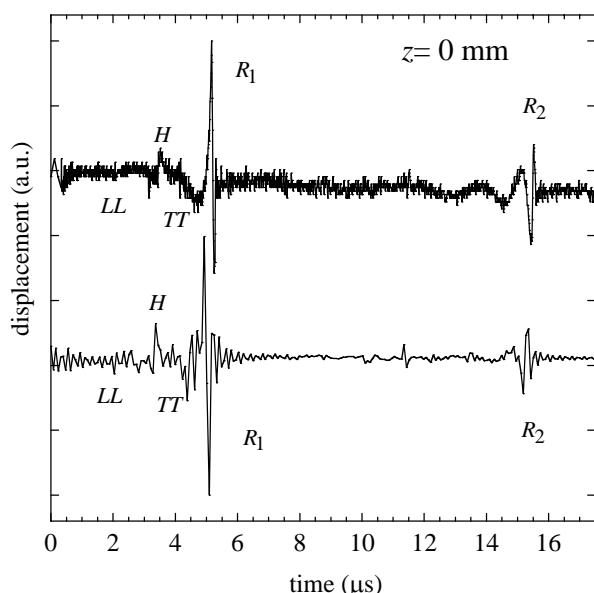
FIG. 4. Experimental (top) and calculated (below) normal displacements at $z=0$ mm of an aluminum cylinder ($2a=9.62$ mm) under thermoelastic regime.

FIG. 5. Experimental (top) and calculated (below) normal displacements at $z=6$ mm of an aluminum cylinder ($2a=9.62$ mm) under thermoelastic regime.

To illustrate the calculation accuracy, normal displacements are obtained and compared at the epicenter ($z=0$) and a non epicenter ($z=6$ mm) positions of the laser point detection for an aluminum cylinder ($2a=9.62$ mm) under thermoelastic regime. The comparisons are shown in Figs. 4 and 5, respectively, where the calculated waveforms are scaled vertically to account for the source magnitude. The arrival time, shape and relative amplitude of each wave are in good agreement. The R_1 and R_2 waves are clearly observed. Their trajectories are shown in Figs. 2(a) and 2(b), respectively, and they have the same shapes and dispersive properties as that generated by the line source[6]. Moreover, the *LL* and the head (*H*) waves are observable. Specifically, the *L* wave is observable at the non epicenter detection (Fig. 5), while it is not visible at the epicenter detection (Fig. 4). This can be explained by the directivity of the thermoelastic generation.

Conclusion

A physical model has been presented to predict the acoustic field generated by a laser point source in either ablation or thermoelastic regime at any point of a homogeneous and isotropic cylinder. Experimental waveforms were measured and identified for either regime. Experimental and theoretical normal displacements under thermoelastic regime are compared for aluminum cylinders. Very good agreements are observed in the time, shape and relative amplitude (i) of the cylindrical Rayleigh waves with different roundtrips, and (ii) of the various longitudinal and transverse bulk waves propagating through the cylinder or reflected at the free circular surface. These results will be helpful in identifying the
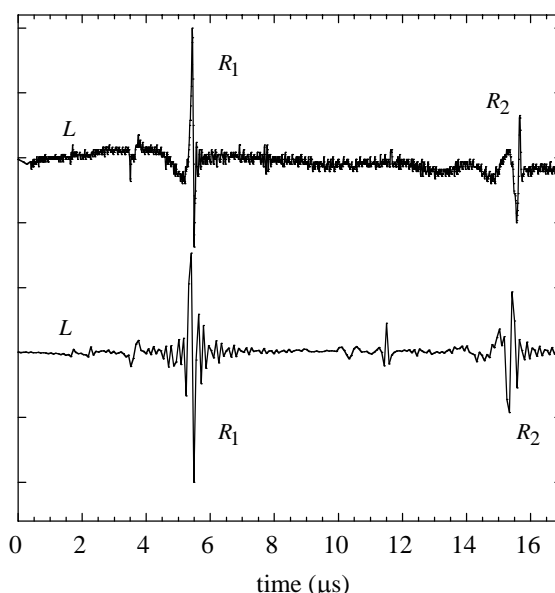
useful wave modes when dealing with the inverse problem for the nondestructive evaluation of cylindrical parts.

References

[1] A. Viktorov, *Rayleigh and Lamb Waves*, Plenum Press, New York, 1967.
[2] H. Uberall, *Physical Acoustics*, Academic, New York, 1973, Vol. 10, p. 1-60.
[3] C. B. Scruby and L. E. Drain, *Laser Ultrasonics: Techniques and Applications*, Adam Hilger, New York, 1990.
[4] D. Royer, E. Dieulesaint, X. Jia, and Y. Shui, "Optical generation and detection of surface acoustic waves on a sphere," Appl. Phys. Lett. **52**, 706-708 (1988).
[5] X. Wu and M. Qian, "Simulation of the finite element method on wave propagation in cylinders," Prog. in Nat. Sci. **11**, s265-s268 (2001).
[6] Y. Pan, C. Rossignol, and B. Audoin, "Acoustic waves generated by a laser line pulse in a transversely isotropic cylinder," Appl. Phys. Lett. **82**, 4379-4381 (2003).
[7] A. Rahman and F. Ahmad, "Representation of the displacement in terms of scalar functions for use in transversely isotropic materials," J. Acoust. Soc. Am. **104**, 3675-3676 (1998).
[8] D. A. Hutchins, *Physical Acoustics* (Academic, New York, 1988), Vol. 18, p. 21-123.
[9] L. R. F. Rose, "Point-source representation for laser-generated ultrasound" J. Acoust. Soc. Am. **75**, 723-732 (1984).
[10] R. L. Weaver, W. Sachse, and K. Y. Kim, "Transient elastic waves in a transversely isotropic plate," J. Appl. Mech. **63**, 337-346 (1996).